



OPEN

Molecular and SEM studies on *Thaparocleidus vistulensis* (Siwak, 1932) (Monopisthocotyla, Ancylo-discoididae)

Wan Muhammad Hazim Wan Sajiri^{1,2}, Csaba Székely¹, Kálmán Molnár¹, Sebastian Kjeldgaard-Nintemann³, Per Walter Kania⁴, Kurt Buchmann⁴ & Boglárka Sellyei¹✉

Presenting new molecular and scanning electron microscope (SEM) features, this study gives additional data to the better knowledge of *Thaparocleidus vistulensis* (Siwak, 1932) (Monopisthocotyla, Ancylo-discoididae), a parasite of the European catfish *Silurus glanis* Linnaeus, 1758 (Siluriformes, Siluridae) cultured in a commercial fish farm in Hungary. In addition, notes on the early development of sclerotized anchors are also provided. The main morphological difference of *T. vistulensis* compared to other congeneric species is associated with the male copulatory organ, which exhibits 5–7 loops in the middle of the penis length and a long open V-shaped sclerotized accessory piece, dividing terminally into two parts, securing the terminal part of the penis tube. The present study provides for the first time molecular characterization data based on the 2694 bp long nucleotide sequence of rDNA (ITS1, 5.8S, ITS2, and flanked with partial 18S and partial 28S) submitted in GenBank with the accession number OR916383. A phylogenetic tree based on ITS1 sequences supports a well-defined clade including *T. vistulensis*, forming a sister group with *T. siluri*, a species-specific monopisthocotylan parasite to *S. glanis*. The morphological characterization of *T. vistulensis*, especially for the male copulatory organ, together with the molecular data in the present study, extends knowledge about this monopisthocotylan species and provides new information for future phylogeny studies.

Keywords *Thaparocleidus vistulensis*, *Silurus glanis*, Sclerotized structure, Male copulatory organ, Molecular analysis, rDNA

Monogeneans are considered the most diverse parasite group with regard to the number of species, morphology, and ecology^{1,2}. These parasites exhibit a high host specificity, parasitizing a single or a narrow group of closely related fishes². Monogenean parasites are equipped with a distinctive posterior attachment structure, the opisthaptor, utilized for anchoring to the host surface (body, fins, and gills). This conspicuous organ is equipped with various types of sclerotized hooks and anchors³, which is, together with sclerotized structures in the male copulatory organ and the vagina, decisive for species differentiation⁴.

Monogenea is considered as a non-monophyletic group based on previous phylogenetic studies including mtDNA⁵ and rDNA⁶. Transcriptomic data studied by Brabec et al.⁷ showed robust and consistent signals in the two non-monophyly monogenean lineages (subclasses: Monopisthocotylea and Polyopisthocotylea). Despite the term use of conventionally recognized as class “Monogenea” being common in the nomenclature of phylum Platyhelminthes, Brabec et al.⁷ proposed to suppress the term and promote the previously subclasses to the class level as Monopisthocotyla new class and Polyopisthocotyla new class. Hence, this terminology will be used here.

Thaparocleidus vistulensis (Siwak, 1932) is a monopisthocotylan ectoparasite occurring on the gills of *Silurus glanis* Linnaeus, 1758. Firstly, it was described by Siwak⁸ from Poland as *Ancyrocephalus vistulensis*. Roman⁹ recorded the species synonym with *Ancylo-discoides siluri*, a synonymization later repeated by Roman-Chiriac¹⁰.

¹HUN-REN Veterinary Medical Research Institute, 21, Hungária Krt, 1143 Budapest, Hungary. ²Doctoral School of Animal Biotechnology and Animal Science (Agricultural Science), Hungarian University of Agriculture and Life Sciences, 1. Páter Károly Str, 2100 Gödöllő, Hungary. ³Center for Advanced Bioimaging, University of Copenhagen, Frederiksberg C, Denmark. ⁴Department of Veterinary and Animal Sciences, Faculty of Health and Medical Sciences, University of Copenhagen, Frederiksberg C, Denmark. ✉email: sellyei.boglarka@vmri.hun-ren.hu

However, it was rejected by Yamaguti¹¹. Several changes of genera occurred until Lim¹² reassessed and transferred them to *Thaparocleidus*. The species was reported infecting the same host (*Silurus glanis*) from Hungary^{13,14}, Czechia^{15,16}, Iraq¹⁷, Iran^{18,19}, Turkey²⁰, Italy^{21,22}, Poland²³, and UK²⁴. In the last century, several descriptions were reported, mainly based on morphological characteristics^{22,25}. Nevertheless, it deserves more attention due to the complicated structure of its male and female copulatory organs.

Although morphological studies form the basis of correct species identification, molecular data is still vital in supporting a complete and conclusive identification²⁶. To date, the description of *T. vistulensis* is based on morphological details and does not provide a molecular characterization of the species described except in²⁷, and the sequence information available at the International Nucleotide Sequence Database Collaboration (INSDC) is limited. This study re-evaluates morphometric data with a specific focus on the haptor and copulatory sclerites, and presents new molecular data and SEM studies, extending current knowledge on the species.

Results

Morphological description

The body is elongated and assumes a cylindrical form but tapers towards the posterior end and terminates with a slightly wider and non-segregated caudal disc (Fig. 1A and 2A–B). The anterior part of the body is extended and flattened, with two pairs of eyespots dorsally, and four pairs of head organs with cephalic glands (Fig. 1B–C). The eyes, aggregation of dispersed pigment spots are located along the vertices of a trapezoid. Adjacent to these pigment spots, positioned at a slightly oblique angle, transparent and intensely refractive corpuscles are discernible (Fig. 1C). The mouth opening is subterminal, and the pharynx, is roundish or short oval, located ventrally in the region behind the eyes (Fig. 1C). The widening haptor region (Fig. 1G) has two pairs—dorsal and ventral—of strong anchors (Fig. 1H–I and 2C–D). The dorsal ones have well-developed inner roots and less prominent outer roots. The ventral anchors have a smaller size, having well-developed inner and outer roots. The dorsal anchors are connected with a straight dorsal bar, while the ventral ones are connected with a V-shaped ventral bar. A small sheet, called a cuneus, was observed joining the inner roots of the dorsal anchors. Both dorsal and ventral anchors are pointed in opposite directions (Fig. 1K–L, 2A–C and 4A–D). The haptor comprises 14 small marginal hooks (Fig. 1J and 2E). All the haptor sclerites are provided with fine chitinous stirrups. The haptor sclerites gripping the gill lamellae of their host can be seen in Fig. 3A–D. Vitellaria are densely dispersed throughout the trunk except in the region of reproductive organs. The testicle is located at the posterior part of the body and is connected with the vas deferens to the seminal vesicle. The seminal vesicle is single, blind-bottomed. The male copulatory organ starts with a flask-shaped bulb usually facing to the right of the ventral body position and connected to a long sclerotized penis tube (Fig. 1D). The flask-shaped bulb has 13.9 ± 0.6 (13.4–15.0) in length and 8.2 ± 1.1 (7.2–10.0) in width. The penis usually has 5–7 loops in the middle of its length before joining the penis accessory. The total length of the penis was 837.4 ± 95.9 (703.6–940.9). The accessory piece of the copulation organ is a sclerotized, open V-shaped structure, composed of a trough-like basal part which receives the penis. Its total length measures 97.0 ± 7.8 (92.5–110.9). In its middle where the accessory part turns to be V-shaped, it splits into two parts. One carries the penis, while the other has an elongated, slightly bent, and somewhat hook-like part that runs parallel before curving back towards the first. We often observed the penis running free on a short section after leaving the accessory piece.

The germarium (Fig. 1E) is anteroventral to the testis (Fig. 1F). Inside the germarium, large ovules with clear nuclei and nucleoli are present in the anterior part, while smaller cells can be seen in the posterior region. The size of the testis and germarium were not measured in the present study.

On the ventral side of the body, the vaginal opening is sinistral (Fig. 2A and 3E) and located above the germarium. The vaginal duct, with a measurement 358.1 ± 39.7 (323.2–409.1), consists of irregular convolutions, connecting to the uterine pore, often forming several loops, and ends at the opening of the seminal receptacle. The terminal part of the vagina forms a muscular chamber that encloses a small chitinous plaque. All features mentioned agree with the initial description of the species (Fig. 4).

Oncomiracidia measure 167.3 ± 7.6 (157.5–177.6) in length and 72.5 ± 4.2 (65–78.4) in width. They have 14 marginal hooks with a length of 15.7 ± 0.7 (14.1–16.7), which are about the same size as those of matured worms. The sickle length was 5.1 ± 0.2 (4.7–5.6). Only an underdeveloped pair of ventral anchors was found in the attaching disc. Their length proved to be 21 ± 1.3 (19.2–22.7), with 2.6 ± 0.1 (2.5–2.8) inner root and 2.6 ± 0.2 (2.4–2.8) outer root.

Remarks

Measurements of the sclerotized parts of organs in general corresponded to data from^{8,25}, and²². Of them⁸, remarked that in young *T. vistulensis* specimens, the pair of ventral anchors appear and grow faster than the dorsal ones, we accept that anchors seen in oncomiracidia belonged to the future ventral anchors. *T. vistulensis* resembles *T. magnus* in the shape of a tube base with a flask-shaped, very long penis with several tubular loops in the middle of the penis, but differs in an accessory piece, where *T. magnus* has the appearance of a tuberos groove with a strongly swollen anterior end, forming three teeth of different shapes¹⁵. We completed the taxonomic characterization with the addition of SEM and histological figures, especially with the morphological description of the oncomiracidia of *T. vistulensis*.

Molecular analysis and phylogenetic tree

In the present study, a 2694 bp long nucleotide sequence including 18S (partial), Internal Transcribed Spacer (ITS) 1, 5.8S, ITS2, and 28S (partial) ribosomal DNA (rDNA) of *Thaparocleidus vistulensis* was obtained. The sequence has been deposited in GenBank under the accession number OR916383. Due to the limited data available in the INSDC, only ITS1 sequences were involved in the phylogenetic analyses. The obtained sequence was then

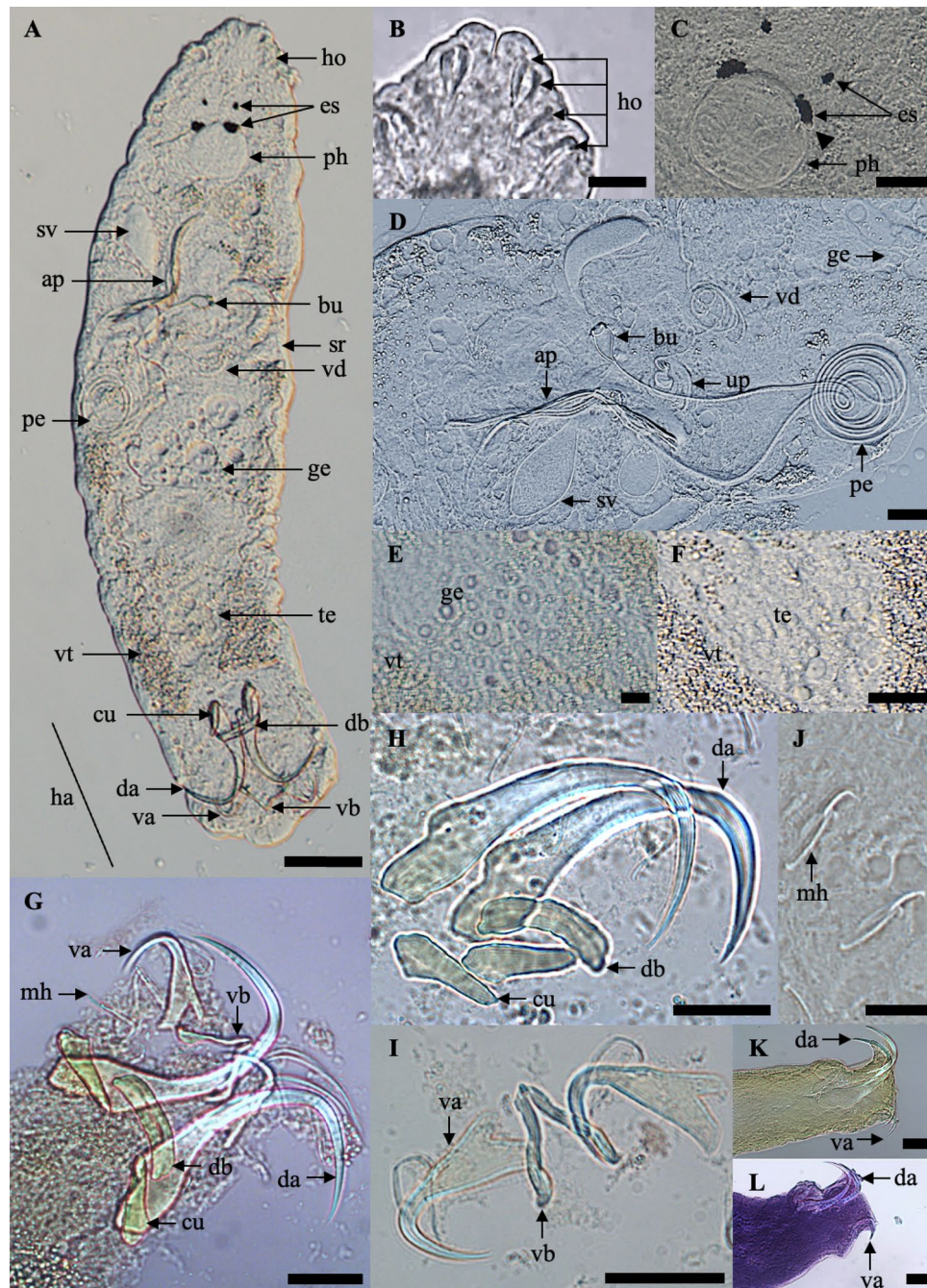


Figure 1. Photomicrograph of *Thaparocleidus vistulensis*. (A) Whole mount—dorsal view; (B–C) Anterior region; (D) Complex internal organ; (E) Germarium; (F) Testis; (G) Opisthaptor; (H) Dorsal anchor with cuneus and dorsal bar; (I) Marginal hooks; (J) Ventral anchor and ventral bar; (K–L) Haptor—lateral view. (A–F) Fresh samples; (G–J) Softened with proteinase K and mounted in glycerine-ammonium-picrate; (K) Mounted in glycerine-ammonium-picrate; (L) Stained with hematoxylin. Abbreviations: ap, accessory piece; bu, bulbous base; cu, cuneus; da, dorsal anchor; db, dorsal bar; es, eye spots; ge, germarium; ha, haptor; ho, head organs; mh, marginal hooks; pe, penis; ph, pharynx; sr, seminal receptacle; sv, seminal vesicle; te, testis; up, uterine pore; va, ventral anchor; vb, ventral bar; vd, vaginal duct; vt, vitellaria. ▲, transparent and intensely refractive corpuscles. Scale bars represent 20 μm , except (A) 100 μm and (J) 10 μm .

compared with previously deposited sequences of the genus *Thaparocleidus*. Our ITS1 sequence shares 97.96% identity with the *T. vistulensis* sequence identified in *Silurus glanis* from the Czechia (AJ490165) and exhibits a 92.18% similarity with *T. siluri* isolated from the same host species and geographical location (AJ490164)²⁷.

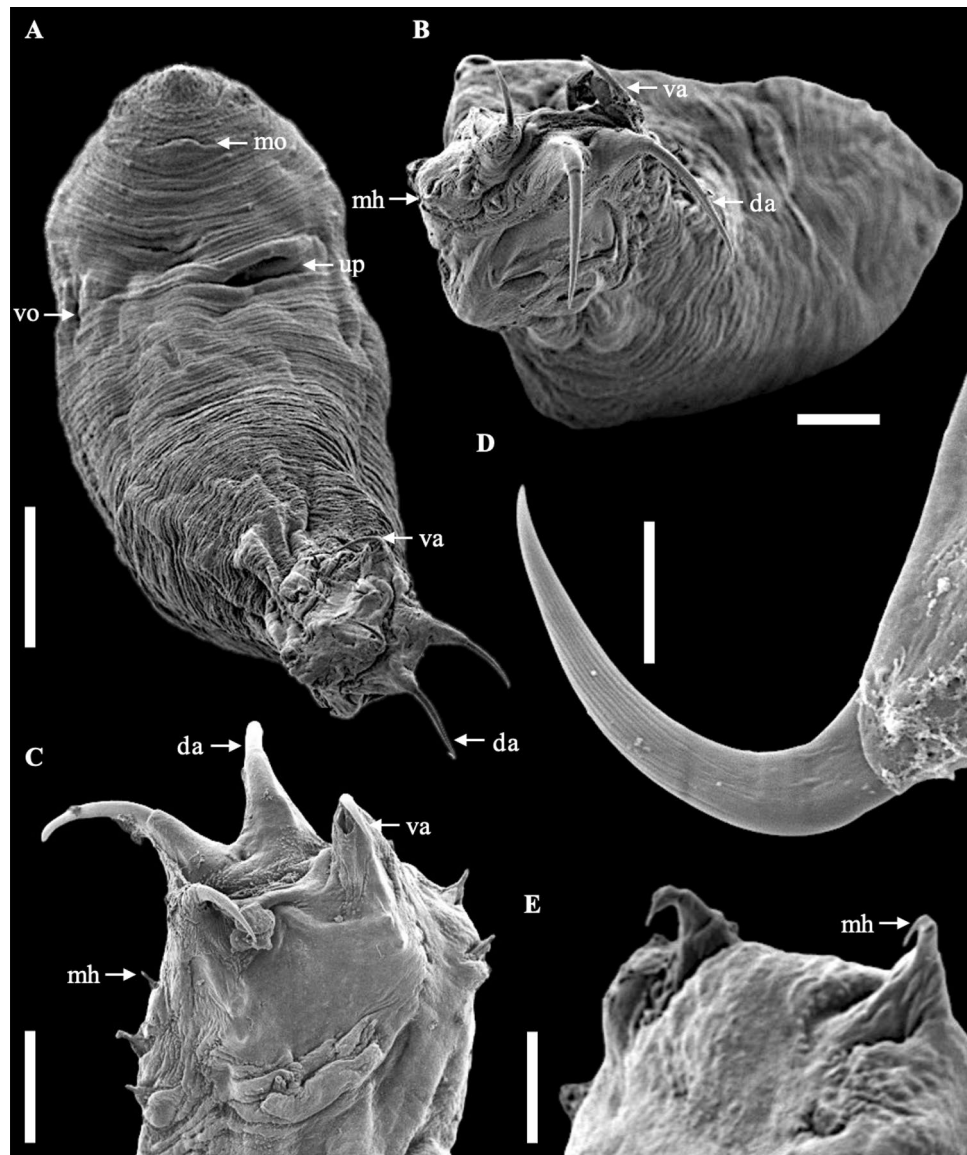


Figure 2. SEM micrographs of *Thaparocleidus vistulensis*. (A) Whole body—ventral view; (B) Whole body—posterior view; (C) Opisthaptor; (D) Dorsal anchor; (E) Marginal hooks. Abbreviations: da, dorsal anchor; mh, marginal hooks; mo, mouth opening; up, uterine pore; va, ventral anchor; vo, vaginal opening. Scale bars represent (A) 50 μm , (B–C) 20 μm , and (D–E) 5 μm .

The (maximum likelihood) ML tree, constructed based on the ITS1 rDNA, robustly supports a well-defined clade that includes the previously identified *T. vistulensis* sequence (Fig. 5). *Thaparocleidus vistulensis* forms a sister group with *T. siluri*, another parasitic species specific to *S. glanis*. Both *T. vistulensis* and *T. siluri* clustered with *T. varicus* and *T. mutabilis* in a distinct branch, and high bootstrap values strongly support this grouping. The sequence variabilities (uncorrected *p* distance) in the ITS1 within genus/species group with *Thaparocleidus vistulensis* were 52.3–98.3% (Supplementary Table 1). Molecular analyses provide compelling evidence that the monopisthocotylian species examined in this study can be confidently attributed to *T. vistulensis*.

Discussion

The three related species (*Thaparocleidus siluri*, *T. vistulensis*, and *T. magnus*) were described from the European catfish by Zandt²⁸, Siwak⁸, and Bychowsky & Nagibina²⁵, respectively. These congeneric species were distinguished by several unique features²⁵. The essential attributes of sclerotized structures, encompassing the haptor parts and copulatory organs – copulatory piece and vagina, remain of paramount importance for species identification and taxonomy^{29–34}. The morphological characteristics of the haptor are regarded as adequate for genus-level parasite identification, while the reproductive organ proves a more suitable clue for species-level discrimination, likely attributable to its higher rate of variability^{31,35,36}. Therefore, it is vitally essential to describe these features and structures meticulously.

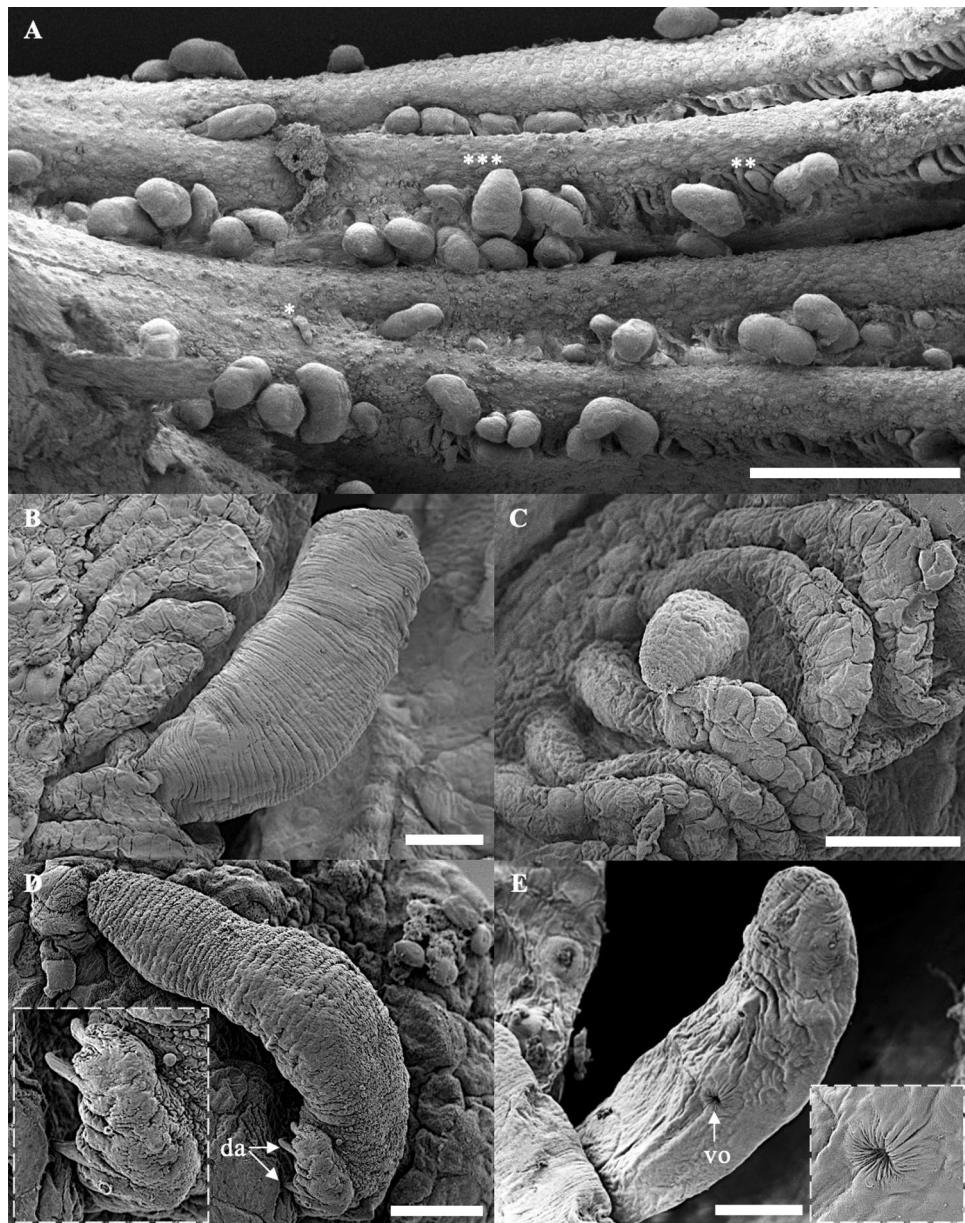


Figure 3. SEM micrographs of *Thaparocleidus vistulensis* are attached to gills lamellae. (A) Extensive hyperplasia of gill filament heavily infected by *T. vistulensis*; (B) Adult *T. vistulensis* with posterior part surrounded by gill tissue—lateral view; (C) Young *T. vistulensis* with posterior part in between gill lamellae—ventral view; (D) Adult *T. vistulensis* penetrating the gill filament—dorsal view; (E) Vaginal opening—ventral view. Abbreviations: da, dorsal anchor; vo, vaginal opening. Asterisks represent (*) Larvae, early stage of attachment, (**) Young, and (***) Adult *T. vistulensis*. Scale bars represent (A) 500 µm, (B, C, E) 50 µm, and (D) 20 µm.

The body size of parasites in this study exhibits a broader range of length (507.1–1002.4) and total body width (120.6–196.2) compared to the literature. This variation can be attributed to the parasites being measured as early as day ten after infection, as indicated by³⁷, who considered them to be in a mature stage. Furthermore, the measured monopisthocotylans were preserved in 80% ethanol for a period before assessment, potentially leading to a size reduction. Nevertheless, the dimensions of each sclerotized feature, specifically the attachment organ, were found to be approximately consistent with the previous study except smaller than those reported by²² (Table 1). This attachment organ suggests that the rigid components of the monopisthocotylan remain fixed and resistant to shrinking.

The male copulatory organ of *T. vistulensis* is a relatively large structure. Hitherto, only a few studies included the dimension size of the copulatory organ studied by light microscopy in whole-mounted specimens^{25,38}. Furthermore, although some of these authors have provided detailed descriptions of an excellent drawing, the exact measurement points are not mentioned, making it sometimes difficult to interpret their descriptions. The present

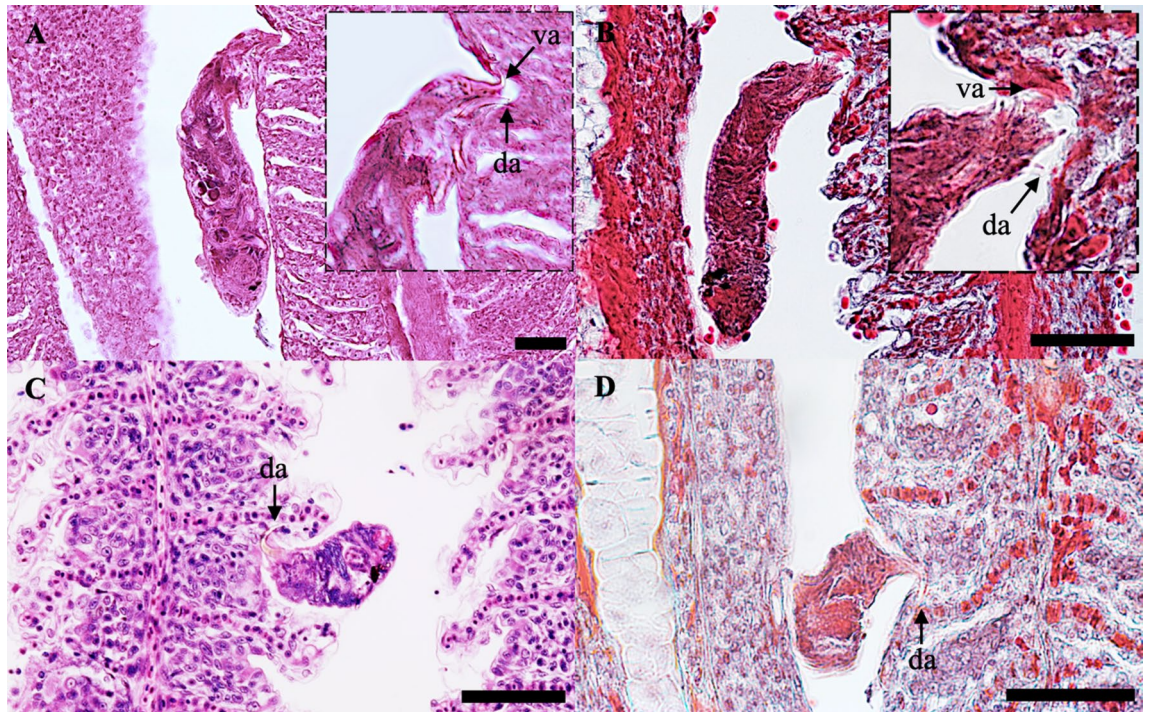


Figure 4. Histological sections of gills attached by *T. vistulensis*. (A–B) Adult *T. vistulensis* with posterior part—anchor inserted and pierced in gill lamellae in the opposite direction; (C–D) Young *T. vistulensis*. Staining method (A, C) stained with H & E; (B, D) stained with Masson–Goldner trichrome staining. Abbreviations: da, dorsal anchor; va, ventral anchor. Scale bars represent 50 μm .

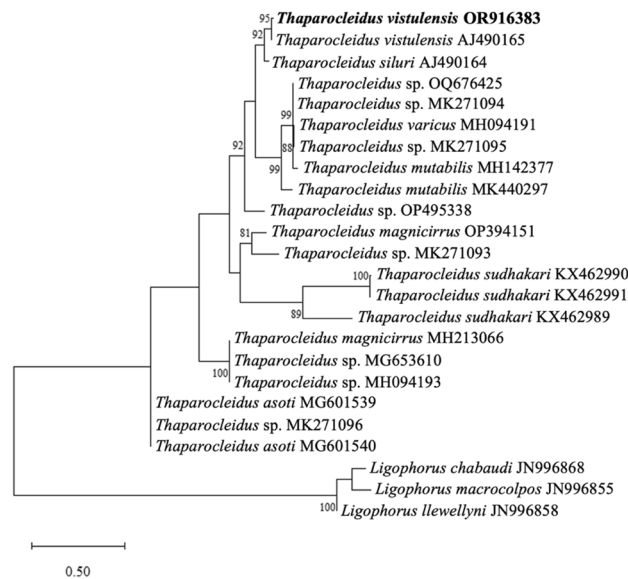


Figure 5. A phylogenetic constructed based on the ITS1 rDNA sequences demonstrating the positions of *Thaparocleidus vistulensis* with other *Thaparocleidus* species. The tree was generated by the ML method and rooted to *Ligophorus* spp. as an outgroup. Numbers at nodes indicate $\geq 80\%$ bootstrap values (1000 replications). Species names are listed along the INSDC accession numbers. Species examined in this study are shown in bold. The scale bar indicates the number of expected substitutions per site.

report of the male copulatory organ is based on light microscopy with a detailed point of measurement on the organ's features, allowing a detailed analysis of the shape.

Assessing from the published drawings, at least eight *Thaparocleidus* species possess a male copulatory organ (i.e., a long thread-like sclerotized penis with coils) similar to that of *T. vistulensis*. This characteristic is shared with several other species, as outlined in Table 2. The overall structure of the male copulatory organ bears a

Morphometric characteristics	Siwak (1932)	Bychowsky and Nagibina (1957)	Paladini et al. (2008) (n=20)	Present Study (n=20)
Body Size *(n=10)				
Total body length	(740.0–1140.0)	(400.0–750.0)	1102.1 ± 167.6 (772.0–1325.6)	691.2 ± 163.0 (507.1–1002.4)
Oncomiracidia	–	–	–	167.3 ± 7.6 (157.5–177.6)
Total body width	(85.0–159.0)	(140.0–270.0)	308.5 ± 48.8 (202.6–360.7)	155.2 ± 27.2 (120.6–196.2)
Oncomiracidia	–	–	–	72.5 ± 4.2 (65–78.4)
Dorsal anchor				
Total length	(70.0–79.0)	(70.0–77.0)	85.8 ± 2.4 (82.8–88.4)	66.2 ± 4.3 (57.6–73.9)
Shaft length	–	(58.0–63.0)	71.7 ± 5.4 (66.2–81.6)	54.5 ± 3.5 (46.9–60.9)
Root length	(18.0–22.0)	(16.0–19.0)	17.7 ± 4.1 (10.5–23.3)	13.9 ± 1.5 (10.9–16.5)
Point length	–	(31.0–35.0)	38.7 ± 3.2 (32.8–41.9)	31.4 ± 2.1 (27.3–35.0)
Aperture	(59.0–68.0)	–	52.8 ± 2.4 (49.1–56.5)	42.8 ± 3.6 (36.4–50.4)
Cuneus				
Total length	(22.0–27.0)	(24.0–28.0)	29.0 ± 2.1 (26.8–32.4)	23.4 ± 1.8 (19.7–26.5)
Largest width	–	(7.0–8.0)	9.7 ± 1.5 (7.6–12.4)	7.8 ± 1.3 (5.8–10.1)
Ventral Anchor				
Total length	(27.0–30.0)	(25.0–28.0)	30.3 ± 2.1 (27.3–32.7)	25.8 ± 1.2 (23.7–27.6)
Oncomiracidia *(n=5) ^a	–	–	–	21 ± 1.3 (19.2–22.7)
Shaft length	–	(21.0–22.0)	25.7 ± 1.3 (23.8–27.6)	21.1 ± 1.0 (19.3–22.6)
Inner root length	–	7.0	8.7 ± 1.46 (7.0–11.2)	6.4 ± 0.6 (5.3–7.9)
Oncomiracidia *(n=5) ^b	–	–	–	2.6 ± 0.1 (2.5–2.8)
Outer root length	–	–	–	5.3 ± 0.4 (4.5–6.0)
Oncomiracidia *(n=5) ^b	–	–	–	2.6 ± 0.2 (2.4–2.8)
Point length	–	(14.0–16.0)	16.2 ± 1.2 (14.3–17.8)	14.9 ± 1.0 (12.1–16.5)
Aperture	(18.0–22.0)	–	20.6 ± 1.6 (18.1–22.7)	18.1 ± 1.4 (16.0–21.2)
Oncomiracidia *(n=5) ^b	–	–	–	14.8 ± 0.3 (14.6–15.3)
Dorsal bar				
Total length	(32.0–37.0)	–	38.4 ± 2.6 (35.1–41.9)	31.6 ± 2.4 (27.1–35.8)
Width in the middle	–	–	9.32 ± 0.7 (8.1–10.0)	6.7 ± 1.2 (5.2–9.9)
Ventral Bar				
Length of one branch	(23.0–25.0)	(23.0–25.0)	25.7 ± 1.5 (23.3–27.5)	21.9 ± 1.4 (19.1–24.4)
Largest width	–	3.0	5.3 ± 0.8 (4.3–6.8)	3.1 ± 0.5 (2.4–4.5)
Marginal Hook *(n=40)				
Total length	16.3	16.0	17.5 ± 0.5 (16.8–17.9)	15.8 ± 0.6 (14.9–16.9)
Oncomiracidia	–	–	–	15.7 ± 0.7 (14.1–16.7)
Sickle length	4.3	–	6.3 ± 0.4 (5.7–6.8)	5.3 ± 0.3 (4.8–5.9)
Oncomiracidia	–	–	–	5.1 ± 0.2 (4.7–5.6)
Male copulatory organ *(n=5)				
Penis	–	640.0	–	837.4 ± 95.9 (703.6–940.9)
No. of loop	–	≥ 4	–	5–7
Accessory piece	–	(68.0–71.0)	–	97.0 ± 7.8 (92.5–110.9)
Farthest point	–	–	–	131.9 ± 20.4 (103.4–156.0)
Bulbous base length	–	(14.0–16.0)	–	13.9 ± 0.6 (13.4–15.0)
Bulbous base width	–	8.0	–	8.2 ± 1.1 (7.2–10.0)
Female copulatory organ *(n=5)				
Vaginal duct	–	≈ 200	–	358.1 ± 39.7 (323.2–409.1)

Table 1. Morphometric characteristics of *Thaparocleidus vistulensis* from the present study and relevant literature. The number of studied parasites and mean values of morphometric characters were not specified in⁸, and²⁵. Mean ± Standard deviation, with range in parentheses. Measurements expressed in micrometers (µm). *Referred to the number of specimens examined in the present study. ^aMorphological part was measured following the anchor curve. ^bMorphological part was measured following ventral anchor parameters in Fig. 6.

resemblance to *T. magnus* and *T. siluri*, characterized by a sclerotized penis tube structure with a flask-shaped bulb, coils in the middle of the length of the penis, and an accompanying accessory piece. However, *T. vistulensis* exhibits a closer affinity to *T. magnus*, but is easily distinguishable based on the male copulatory organ (i.e., distant points of the copulatory organ) other than the size of body and attachment structure²⁵.

In certain instances, taxonomic identification presents challenges at both generic and specific taxonomic levels. As a result, molecular identification emerges as a valuable tool for clarifying taxonomic issues, especially

Species	Total length	Total coils	References
Genus <i>Thaparocleidus</i> Jain 1952			
<i>T. armillatus</i> Verma, Chaudhary and Singh, 2017	82–89	1.5	51
<i>T. devraji</i> Gusev, 1976	93–133	1.5	52
<i>T. magnus</i> Bychowsky and Nagibina, 1957	1400–1600	*	25
<i>T. malabaricus</i> Gusev, 1976	*	3.5	53
<i>T. seenghali</i> Jain, 1961	*	2–3	53
<i>T. siluri</i> Zandt, 1924	390–420	2–3	25
<i>T. susanae</i> Rajvanshi & Agrawal, 2013	193–198	3	54
<i>T. wallagonius</i> Jain, 1952	*	3–4	51
Genus <i>Demidospermus</i> Suriano, 1983			
<i>D. spirophallus</i> Franceschini, Zago, Müller, Francisco, Takemoto & da Silva, 2017	193–230	2.5	26
<i>D. prolixus</i> Franceschini, Zago, Müller, Francisco, Takemoto & da Silva, 2017	210–234	1.5	26
<i>D. anus</i> Suriano, 1983	143–156	1–1.5	26
Genus <i>Mastacembelocleidus</i> Kritsky, Pandey, Agrawal & Abdullah, 2004			
<i>M. bam</i> Tripathi, 1959	*	2	55
<i>M. heteranchorus</i> Kulkarni, 1969	*	2	55
Genus <i>Dactylogyrus</i> Diesing, 1850			
<i>D. nasutai</i> Narba, Matey, Agarwal & Tripathi, 2022	*	27	56
<i>D. pulcher</i> Bychowsky, 1957	250	6–7	39
<i>D. simplicimalleata</i> Bychowsky, 1931	340	*	39
<i>D. wuhuensis</i> Lee, 1960	155–185	2.5–3	39
<i>D. falciformis</i> Akhmerov, 1952	190–220	3	39
<i>D. procypris</i> Ma, Li & Wang, 1981	360	*	57
<i>D. longivagina</i> Zhang & Pan, 1988	410–610	6–8	57
<i>D. pseudoflagillicirrus</i> Long, 1964	300	*	57
<i>D. luciosomis</i> Zhang & Guo, 1981	80–140	*	57
<i>D. sphyrna</i> Linstow, 1878	90–98	*	57
<i>D. onychocirrus</i> Long, 1981	88–110	*	57
<i>D. lingualis</i> Long, 1981	114–125	3	57
<i>D. rhychoideus</i> Long, 1981	122	2	57
<i>D. spirovagina</i> Long, 1981	71	2	57
<i>D. longquanensis</i> Wu & Wang, 1983	199–282	1–2	57
<i>D. quadricurvitubus</i> Zhang & Guo, 1982	165–235	4–7	57
<i>D. austrosinensis</i> Zhang & Li, 1991	190–207	2	57
<i>D. strombus</i> Tao & Long, 1981	340–660	4–11	57
<i>D. daojiensis</i> Luo & Long, 1982	376	*	57
<i>D. pectinate</i> Zhao & Ma, 1991	174–177	2	57
<i>D. ehrenbergii</i> Yao & Wang, 1997	149–210	2	57
<i>D. garrae</i> Ma & Long, 2000	167–185	7	57
<i>D. lianshanensis</i> Ma & Long, 2000	120–207	*	57
<i>D. helicoides</i> Yao & Wang, 1997	376–1455	4–10	57
Genus <i>Pseudacolpenteron</i> Bychowsky & Gusev, 1955			
<i>P. ignotus</i> Gussev, 1955	190	2	39
Genus <i>Ancyrocephalus</i> Creplin, 1839			
<i>A. subaequalis</i> Akhmerov, 1952	130–170	*	39
<i>A. pavlovskiyi</i> Gussev, 1955	140–160	*	39
<i>A. brevifilis</i> Yao & Wang, 1997	248–348	*	57
Genus <i>Dogielius</i> Bychowsky, 1936			
<i>D. strombicinms</i> Ma & Long, 2000	357	7	57
Genus <i>Pseudancylodiscooides</i> Yamaguti, 1963			
<i>P. panduriformis</i> Zhang & Ma, 1997	116–149	1.5	57

Table 2. List of freshwater monopisthocotylan parasites with long penis and coils based on published drawings. *Data not provided.

when morphological distinctions among monopisthocotylan genera or species groups are ambiguous^{31,35,36}. The phylogenetic analysis clustered the *T. vistulensis* sequence obtained in this study (Fig. 5) together with other *Thaparocleidus* spp. that have shown the highest nucleotide similarities via a BLAST search.

In the present study, a 2694 bp-long fragment, including partially 18S, ITS, 5.8S, and partially 28S rDNA of the monopisthocotylan (accession number OR916383), was successfully sequenced. A lack of available *Thaparocleidus* species sequences covering all these gene markers in the GenBank prevented the alignment of the whole sequence generated. Therefore, a part of the obtained sequence was removed before analysis, and only ITS1 was used for the comparison. The ITS1 sequences of two *T. vistulensis* isolates from the current and previous studies (AJ490165) are found to be closely related to each other. In the phylogenetic tree, both isolates branched at a single nodal point well supported by high bootstrap, proving they belong to the same species. *T. siluri* was found to be a sister species to *T. vistulensis*. This clade comprises *Thaparocleidus* species that have been reported to infect *S. glanis*^{25,39}.

Based on the morphological characterization and molecular analysis of the ITS1, we can conclude that the studied monopisthocotylan species is *T. vistulensis*, which was previously widely reported to infect *S. glanis*. This study provides a redescription for *T. vistulensis*, particularly for the characterization of the male copulatory organ, combined with the molecular data for species identification. To better understand this monopisthocotylan parasite, further studies on multiple parasite specimens and genetic markers are needed. In addition, the pathogen-specific effect of *T. vistulensis* on the host gills would be worth discussing in a forthcoming study, as to our knowledge, no information on this is currently available in the literature, except for Molnár⁴⁰.

Methods

Ethical statement

The experimental protocols together with fish handling and sampling were approved by the Institutional Animal Care and Use Committee of the Veterinary Medical Research Institute, Budapest, Hungary. All research involving experiments on fish (European catfish) was reviewed and approved by the Hungarian National Scientific Ethical Committee on Animal Experimentation under reference number: PE/EA/00081-4/2023. The authors complied with the ARRIVE guidelines (<https://arriveguidelines.org>).

Collection of fish and parasites

Naturally infected European catfish with *Thaparocleidus vistulensis*, obtained from a commercial fish farm in Hungary, were transported to the Veterinary Medical Research Institute in Budapest, Hungary (HUN-REN VMRI), maintained at 23 ± 1 °C in a flow-through tank system, and subjected to a parasitological investigation. Upon arrival at the institute, gill biopsies were procured from the first gill arch using dissection scissors⁴¹ to confirm the presence of parasites. The parasite population was then maintained by co-habitation according to the method of⁴², and the adult and larval (oncomiracidia) parasites were collected following³⁷. All life stages of monopisthocotylan were fixed in 80% ethanol and 5% formalin. Some parasites were freshly recovered and studied alive, but additional samples, left and right sides of excised gill arches, were preserved in 80% ethanol or 5% formalin, respectively, until further use.

Morphological analysis

Some parasites were softened and cleared in a mild enzymatic digestion proteinase K, modifying the method described by⁴³, before mounted individually in 1–2 drops of glycerine-ammonium-picrate on a slide (depending on the size of specimens)⁴⁴. The preparation was then covered with a coverslip. Some specimens were stained using hematoxylin (Harris' modified solution, Sigma-Aldrich HHS32), mounted on a glass slide using AQUA-TEX® (cat. no. HC568794, Merck), and covered by a coverslip.

Photomicrographs were performed using a digital camera (Leica MC170 HD) with LAS V4.12 software equipped with a light microscope (Leica DM5000B Microscope W/ CTR5000 Controller). Subsequently, line drawings of the monopisthocotylan's important part (e.g., the sclerotized structure of the haptor and the male copulatory complex) were made based on the photos. The measurements were made and analyzed based on the captured images using the scientific image analysis tool—ImageJ 1.53t software (RRID: SCR_003070). The morphological parameters of monopisthocotylan, including the sclerotized structure and male copulatory organ, were measured as proposed by⁴⁵ and²² (Figs. 6 and 7). These measurements (Table 1) were presented as mean with standard deviation followed by the range in parenthesis, provided in micrometers (µm). Measurements were conducted of adult parasites: total body width and length ($n = 10$), each of attachment structures ($n = 20$), marginal hooks ($n = 40$), and copulatory organs ($n = 5$). Structures of oncomiracidia ($n = 5$) (except for marginal hooks) were measured as well. Data obtained from this study were compared with the previous descriptions by^{8,25}, and²².

Scanning electron microscope (SEM)

The parasites that were previously preserved in 5% formalin were transferred in Karnovsky's fixative (4% paraformaldehyde and 2% glutaraldehyde in 0.1 M sodium cacodylate buffer) for 15-min, then rinsed in 0.1 M sodium cacodylate buffer two times for 20-min, before immersed in demineralized water two times for 15-min. The samples were then dehydrated through the ascending concentrations of ethanol series (20, 30, 50, 70, 90, 90, 100, and 100%) for 15-min per treatment, except 100% (30-min per treatment). Samples were subsequently dried by passing into 100% hexamethyldisilazane (HMDS) (cat. no. 52620, Fluka) for 30-min and set aside in a fume hood overnight. The dehydrated samples were attached to a strip of carbon conductive double-sided tape that was fixed to an SEM aluminum stub. Then, the samples were sputter coated with gold in Leica EM ACE200 Vacuum Coater (Leica, Wetzlar, Germany) with a thickness of 5–10 nm and examined in an FEI Quanta 200 SEM

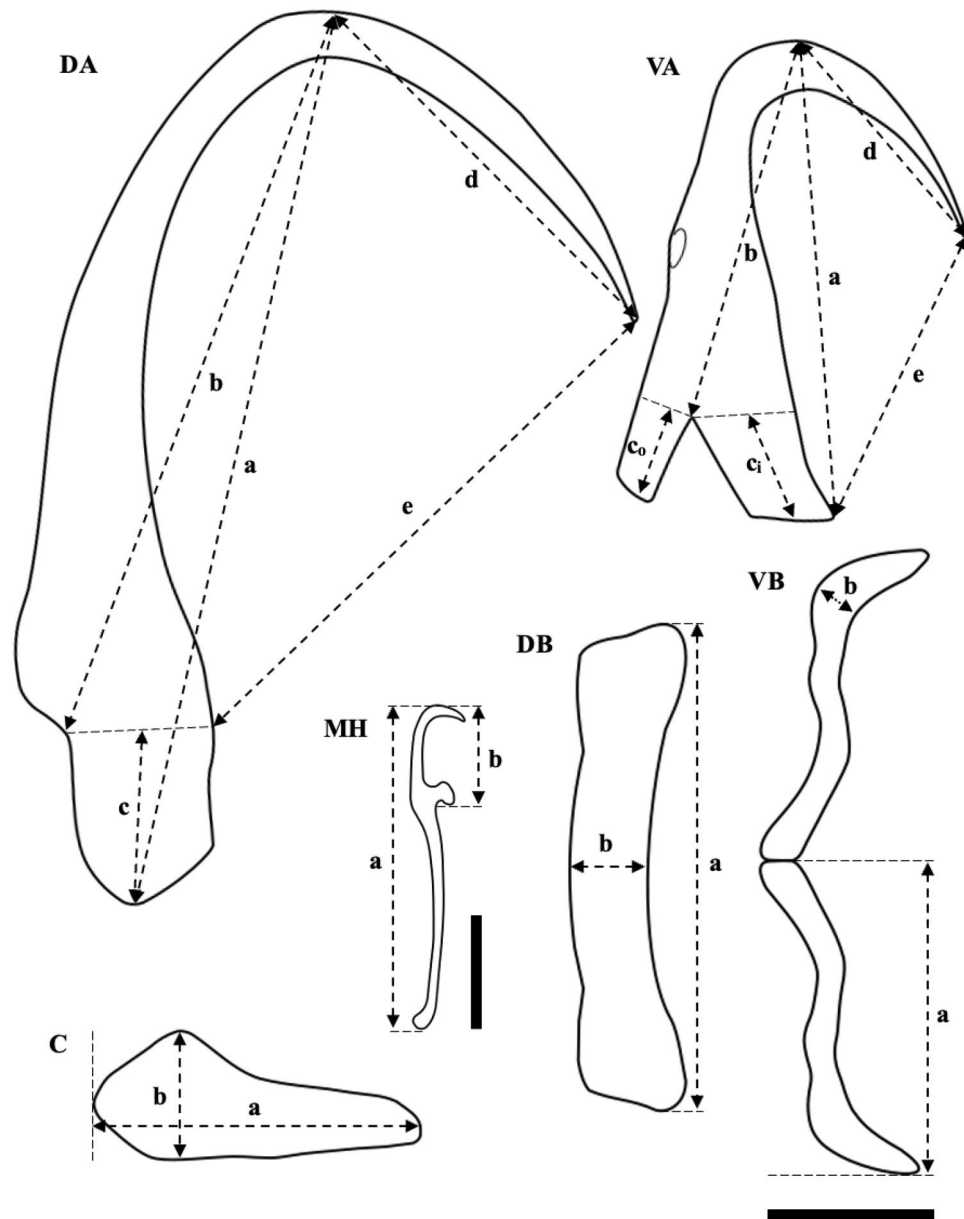


Figure 6. Metric parameters of the *Thaparocleidus vistulensis* attachment apparatus used in this study. Abbreviations: C, cuneus (a, total length; b, largest width); DA, dorsal anchor (a, total length; b, shaft length; c, root length; d, point length; e, aperture); DB, dorsal bar (a, total length; b, width in the middle); MH, marginal hooks (a, total length; b, sickle length); VA, ventral anchor (a, total length; b, shaft length; c_i , inner root length; c_o , outer root length; d, point length; e, aperture); VB, ventral bar (a, length of one branch; b, largest width). All parts of anchors refer to a scale bar of 10 μm , except for the marginal hooks, with a scale bar of 5 μm . The terminology and methodology of measurements are according to^{29,50}, and²².

(FEI Company, Hillsboro, Oregon, United States) operating at 3–8 kV acceleration voltage, using xT Microscope Control software.

Histology

For histology, the gills arch infected with monopisthocotylans that were previously fixed in 5% formalin solution were processed by standard histology techniques, dehydrated in a series of ethanol (70, 96, 100%) and xylol baths, embedded in paraffin wax for cross sections at a 5 μm thickness using a microtome (Leica RM2135, Germany). Sections were deparaffinized before being stained with hematoxylin–eosin (H&E) and Masson–Goldner trichrome staining. Histological sample sections were observed under a light microscope.

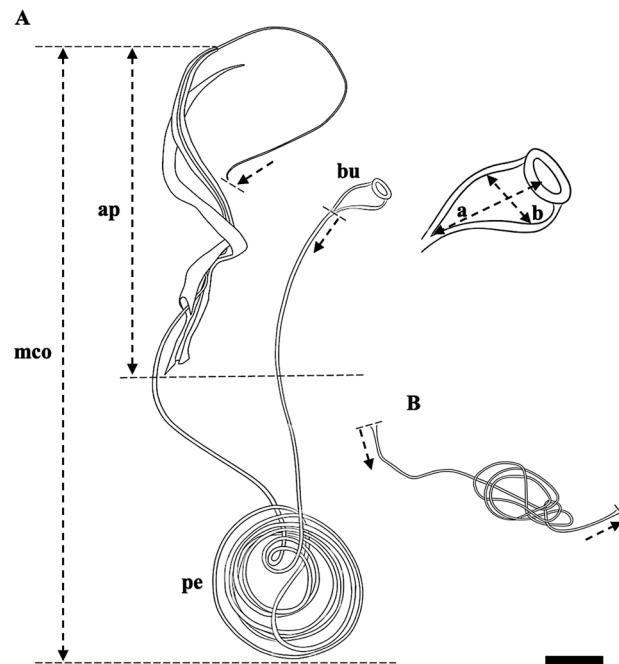


Figure 7. Measurements of the male copulatory organ. (A) Male copulatory organ; (B) Vaginal duct. Abbreviations: ap, total length of accessory piece; bu, bulbous base (a, total length; b, largest width); mco = distal end points of the male copulatory organ; pe, total length of penis (|→ = starting point, →| = ending point). Scale bar represents 20 μm .

Molecular identification and phylogenetic analyses

Species identification of monopisthocotylans was confirmed by molecular methods, PCR and sequencing. Adult monopisthocotylans that were preserved in 80% ethanol were used. The DNA of the specimen was extracted using a QIAamp[®] DNA Mini Kit (250) (cat. no. 51306, Qiagen, Denmark) according to the manufacturer's protocol with a final elution volume of 50 μl . The extracted DNA (2 μl) was subsequently quantified using a NanoDrop (ND-1000) spectrophotometer (Thermo Fisher Scientific, Wilmington, DE, USA). The ITS rDNA fragment encompassing ITS1, 5.8S, ITS2 and flanked with 18S and 28S rDNA genes were amplified with primers PDG_18S_F5 (5'-CGA TAA CGA ACG AGA CTC-3') (in house primer) and NLR1270 (5'-TTC ATC CCG CAT CGC CAG TTC-3')⁴⁶. The PCR amplification was performed on a T100 Thermal Cycler (Bio-Rad, Hercules, CA, USA) with a total volume of 60 μl reaction mixture containing 6 μl sample DNA, 6 μl for each primer (10 mM), 6 μl 10 \times NH₄ buffer, 1.8 μl MgCl₂ (50 mM), 0.6 μl DNA polymerase 5 U/ μl (cat. no. BIO-21060, Nordic BioSite, Denmark), 6 μl dNTP's (10 mM) (cat. no. 4303442 Thermo Fisher Scientific, Denmark), and UltraPure[™] DNase/RNase-Free Distilled Water (cat. no. 10977049, Thermo Fisher Scientific, Denmark)⁴⁷. The PCR reaction conditions were 5-min at 94 °C for initial denaturation, followed by 45 cycles of denaturation at 94 °C for 30-s, annealing at 54 °C for 30-s, extension at 72 °C for 2.5-min, with a final extension step at 72 °C for 7-min, and an indefinite hold at 4 °C. The PCR product was expected to be 2694 bp. The PCR product was separated by gel electrophoresis in 1.5% agarose (cat. no. 10264544, Thermo Fisher Scientific, Denmark) Tris-acetate-EDTA (TAE) gel containing ethidium bromide stain alongside 5 μl of a 50 bp DNA Hyperladder[™] (cat. no. BIO-33040, Nordic BioSite, Denmark), and the amplified DNA fragment was visualized under Azure 200 Gel Imaging Workstation (Azure Biosystems, Dublin, California, USA). The PCR product was purified using Illustra[™] GFX[™] PCR and Gel band purification kit (VWR International, Denmark), and sequencing was performed at Macrogen Europe BV (Amsterdam, Netherlands) using the same PCR primers. Sequences obtained were analyzed using CLC Main Workbench v20.0.4 software (Qiagen, Denmark). Afterwards, the sequence was confirmed by BLAST analysis at the National Center for Biotechnology Information (NCBI) platform. The sequence was then submitted to GenBank. For the phylogenetic analysis, only the ITS1 sequence region was selected due to limited data availability for other parts of the rDNA of *Thaparocleidus* spp. in the INSDC. For molecular comparison, 20 ITS1 sequences of related species were chosen from the databases. Sequences were aligned using ClustalW algorithm in MEGA 11⁴⁸. The phylogenetic tree was performed by the ML method using the general time-reversible (GTR + G + I) substitution model according to the Akaike information criterion (AIC) in MEGA 11⁴⁹. Bootstrap analysis with 1000 replicates was applied to estimate nodal support. The analysis involved 24 nucleotide sequences with a total of 293 positions in the final data sets for the ITS1 gene marker. Sequences of *Ligophorus llewellyni* (JN996858), *Ligophorus chabaudi* (JN996868) *Ligophorus macrocolpos* (JN996855) were used to root the phylogenies. Level of sequence variation based on uncorrected pairwise distance (*p* distance) was calculated using MEGA 11⁴⁸.

Data availability

Raw sequencing data that support the findings of this study have been deposited to the database of NCBI with accession number OR916383, while the datasets generated and analysed during the current study are available from the corresponding author on reasonable request.

Received: 12 February 2024; Accepted: 30 April 2024

Published online: 04 May 2024

References

- Poulin, R. The evolution of monogenean diversity. *Int. J. Parasitol.* **32**, 245–254 (2002).
- Thatcher, V. E. *Aquatic biodiversity in Latin America: Amazon fish parasites* 2nd edn, 508 (Pensoft, 2006).
- Loker, E. S. & Hofkin, B. V. *Parasitology—A conceptual approach* 1–560 (Taylor Francis, New York, 2015).
- Řehulková, E., Seifertová, M., Příkrylová, I. & Francová, K. Monogenea. In: Scholz, T., Vanhove, M. P. M., Smit, N., Jayasundera, Z. & Gelnar, M. (eds) *A Guide to the Parasites of African Freshwater Fishes*. CEBioS, Royal Belgian Institute of Natural Sciences: Brussels, Belgium, **18**, 185–243 (2018).
- Perkins, E. M., Donnellan, S. C., Bertozzi, T. & Whittington, I. D. Closing the mitochondrial circle on paraphyly of the Monogenea (Platyhelminthes) infers evolution in the diet of parasitic flatworms. *Int. J. Parasitol.* **40**, 1237–1245 (2010).
- Laumer, C. E. & Giribet, G. Inclusive taxon sampling suggests a single, stepwise origin of Ectolecithality in Platyhelminthes. *Biol. J. Linn. Soc. Lond.* **111**, 570–588 (2014).
- Brabec, J., Salomaki, E. D., Kolisko, M., Scholz, T. & Kuchta, R. The evolution of endoparasitism and complex life cycles in parasitic platyhelminths. *Curr. Biol.* **33**(19), 4269–4275 (2023).
- Siwak, J. *Ancyrocephalus vistulensis* sp. n., un nouveau trématode, parasite du silure (*Silurus glanis* L.). *Bull. Int. Acad. Polon. Sci., Cl. Sci. Math., Ser. B, Sci. Nat.* **11**(7–10), 669–679 (1932).
- Roman, E. Contribuții la cunoașterea faunei de monogenee din R.P.R. *Bull. Stiintific* **5**(4), 807–831 (1953).
- Roman-Chiriac, E. Fauna republicii populare romineine: Plathelminthes volumul II fascicula 1: Clasa monogeneoidea. Editura Academiei Republicii Socialiste România, Bucharest, pp 150 (1960).
- Yamaguti, S. *Systema helminthum*, vol. IV: *Monogenea and Aspidocotylea*. Intersci. Publ., New York, pp 699 (1963).
- Lim, L. H. S. *Thaparocleidus* Jain, 1952, the senior synonym of *Silurodiscoides* Gussev, 1976 (Monogenea: Ancylo-discoidinae). *Syst. Parasitol.* **35**(3), 207–215 (1996).
- Papp, A. *Gill disease of sheatfish*. *Halász* **2**, 106–107 (1955) (In Hungarian).
- Molnár, K. Worm disease (Ancylo-discoidosis) in catfish (*Silurus glanis*). *Z. Fisheries NF* **16**, 31–41 (1968) (In German).
- Ergens, R. & Lom, J. *Causative agents of fish diseases* 383 (Prague, Academia Praha, 1970).
- Moravec, F. *Checklist of the metazoan parasites of fishes of the Czech Republic and the Slovak Republic (1873–2000)*. Academia Praha, Prague, pp 168 (2001).
- Rahemo, Z. I. F. & Al-Naeime, B. S. Parasites of the freshwater fish, *Silurus glanis*, captured from Tigris River, Mosul, Iraq. Third International Symposium on Aquatic Animal Health, August 30– September 3, 1998, Baltimore, USA: Poster no 99 (1998).
- Roohi, J. D., Sattari, M., Asgharnia, M. & Rufchaei, R. Occurrence and intensity of parasites in European catfish, *Silurus glanis* L., 1758 from the Anzali wetland, southwest of the Caspian Sea Iran. *Croat. J. Fish* **72**(1), 25–31 (2014).
- Khara, H. & Sattari, M. Occurrence and intensity of parasites in Wels catfish, *Silurus glanis* L. 1758 from Amirkelayeh wetland, southwest of the Caspian Sea. *J. Parasit. Dis.* **40**, 848–852 (2016).
- Soylu, E. Metazoan parasites of catfish (*Silurus glanis* Linnaeus, 1758) from Durusu (Terkos) Lake. *J. Black Sea/Medit Environ.* **11**, 225–237 (2005).
- Galli, P., Stefani, F., Benzoni, F., Crosa, G. & Zullini, A. New records of alien monogeneans from *Lepomis gibbosus* and *Silurus glanis* in Italy. *Parassitologia* **45**(3–4), 147–149 (2003).
- Paladini, G., Gustinelli, A., Fioravanti, M. L., Minardi, D. & Prearo, M. Redescription of *Thaparocleidus vistulensis* (Monogenea: Ancylo-discoididae) from Wels catfish (*Silurus glanis* L.) from Po river and taxonomic status of the genus. *Ittiopatologia* **5**, 129–138 (2008).
- Sobecka, E., Wierzbicka, J. & Hatupka, M. A comparative study on the parasite fauna of wels catfish *Silurus glanis* (L.) from a heated water - channel fish farm and a natural water body. *Bull. Eur. Assoc. Fish Pathol.* **30**(1), 8–14 (2010).
- Reading, A. J., Britton, J. R., Davies, G. D., Shinn, A. P. & Williams, C. F. Introduction and spread of non-native parasites with *Silurus glanis* L. (Teleostei: Siluridae) in UK fisheries. *J. Helminthol.* **86**(4), 510–513 (2012).
- Bychowsky, B. E. & Nagibina, L. F. Monogenetic trematodes of *Silurus glanis*. *Parasitol. Sb. Zoological Institute of the Russian Academy of Sciences* **17**, 235–250 (1957).
- Franceschini, L. *et al.* Morphology and molecular characterization of *Demidospermus spirophallus* n. sp., *D. prolixus* n. sp. (Monogenea: Dactylogyridae) and a redescription of *D. anus* in siluriform catfish from Brazil. *J. Helminthol.* **92**(2), 228–243 (2018).
- Šimková, A., Plaisance, L., Matějsová, I., Morand, S. & Verneau, O. Phylogenetic relationships of the Dactylogyridae Bychowsky, 1933 (Monogenea: Dactylogyridae): the need for the systematic revision of the Ancyrocephalinae Bychowsky, 1937. *Syst. Parasitol.* **54**, 1–11 (2003).
- Zandt, F. *Fischparasiten des Bodensees* (Doctoral dissertation, Fischer). *Z. Bakteriolog. Parasitenkd. Infekt.* **92**, 225–271 (1924).
- Gussev, A. V. Monogenea. In *Key to the parasites of the freshwater fish fauna of the USSR* (ed. Bauer, O. N.) Nauka, Leningrad, **2**, 1–268 (1985). (In Russian)
- Wu, X. Y., Chilton, N. B., Zhu, X. Q., Xie, M. Q. & Li, A. X. Molecular and morphological evidence indicates that *Pseudorhabdosynochus lantauensis* (Monogenea: Diplectanidae) represents two species. *Parasitol.* **130**(6), 669–677 (2005).
- Pouyaud, L., Desmarais, E., Deveney, M. & Pariselle, A. Phylogenetic relationships among monogenean gill parasites (Dactylogyridae, Ancyrocephalidae) infesting tilapiine hosts (Cichlidae): systematic and evolutionary implications. *Mol. Phylogenet. Evol.* **38**(1), 241–249 (2006).
- Mendlová, M., Desdevises, Y., Cívánová, K., Pariselle, A. & Šimková, A. Monogeneans of West African cichlid fish: Evolution and cophylogenetic interactions. *PLoS One* **7**(5), e37268 (2012).
- Řehulková, E., Mendlová, M. & Šimková, A. Two new species of Cichlidogyrus (Monogenea: Dactylogyridae) parasitizing the gills of African cichlid fishes (Perciformes) from Senegal: morphometric and molecular characterization. *Parasitol. Res.* **112**, 1399–1410 (2013).
- Khang, T. F., Soo, O. Y. M., Tan, W. B. & Lim, L. H. S. Monogenean anchor morphometry: Systematic value, phylogenetic signal, and evolution. *PeerJ* **4**, e1668 (2016).
- Wu, X. Y., Zhu, X. Q., Xie, M. Q. & Li, A. X. The evaluation for generic-level monophyly of Ancyrocephalinae (Monogenea, Dactylogyridae) using ribosomal DNA sequence data. *Mol. Phylogenet. Evol.* **44**(2), 530–544 (2007).
- Wu, X. Y., Zhu, X. Q., Xie, M. Q., Wang, J. Q. & Li, A. X. The radiation of *Thaparocleidus* (Monogenea: Ancylo-discoidinae): phylogenetic analyses and taxonomic implications inferred from ribosomal DNA sequences. *Parasitol. Res.* **102**, 283–288 (2008).

37. Wan Sajiri, W. M. H., Székely, C., Molnár, K., Buchmann, K. & Sellyei, B. Reproductive strategies of the parasitic flatworm *Thaparocleidus vistulensis* (Siwak, 1932) (Platyhelminthes Monogenea) infecting the European catfish *Silurus glanis* Linnaeus, 1758. *Int. J. Parasitol. Parasites Wildl.* **22**, 113–120 (2023).
38. Abdullah, S. M. A. & Shwani, A. A. A. Ectoparasites of the Asian catfish *Silurus triostegus* (Heckel, 1843) from Greater Zab river-Kurdistan region-Iraq. *J. Duhok. Univ.* **13**(1), 164–171 (2010).
39. Pugachev, O. N., Gerashev, P. I., Gushev, A. V., Ergens, R. & Khotenowsky, I. *Guide to Monogeneoidea of freshwater fish of Palaearctic and Amur Regions*. Ledizioni-Ledipublishing, Milano, pp 562 (2010).
40. Molnár, K. A histological study on ancylostidiosis in the sheatfish (*Silurus glanis*). *Helminthologia* **17**, 117–126 (1980).
41. Gushev, A. V. Methods for collecting and processing fish parasitic monogenean material, 1st edn. Akad Nauk USSR, Leningrad, pp 48 (1983). (In Russian)
42. Hutson, K. S., Brazenor, A. K., Vaughan, D. B. & Trujillo-González, A. Monogenean parasite cultures: Current techniques and recent advances. *Adv. Parasitol.* **99**, 61–91 (2018).
43. Harris, P. D. & Cable, J. *Gyrodactylus poeciliae* n. sp. and *G. milleri* n. sp. (Monogenea: Gyrodactylidae) from *Poecilia caucana* (Steindachner) in Venezuela. *Syst. Parasitol.* **47**, 79–85 (2000).
44. Malmberg, G. On the occurrence of *Gyrodactylus* on Swedish fish. *Skrifter Utgivna av Södra Sveriges Fiskeriförening Arsskrift* 19–76 (1957).
45. Gushev, A. V. Class Monogeneoidea. In *Key to parasites of freshwater fish of the USSR* (eds Bychovskaya-Pavlovskaya, I. E. et al.) 919 (Akad Nauk SSSR, Moscow-Leningrad, 1962).
46. Bartošová, P., Fiala, I. & Hypša, V. Concatenated SSU and LSU rDNA data confirm the main evolutionary trends within myxosporeans (Myxozoa: Myxosporidia) and provide an effective tool for their molecular phylogenetics. *Mol. Phylogenet. Evol.* **53**(1), 81–93 (2009).
47. Zuo, S., Kania, P. W., Mehrdana, F., Marana, M. H. & Buchmann, K. *Contraecium osculatum* and other anisakid nematodes in grey seals and cod in the Baltic Sea: Molecular and ecological links. *J. Helminthol.* **92**(1), 81–89 (2018).
48. Tamura, K., Stecher, G. & Kumar, S. MEGA11: Molecular evolutionary genetics analysis version 11. *Mol. Biol. Evol.* **38**, 3022–3027 (2021).
49. Nei, M. & Kumar, S. *Molecular Evolution and Phylogenetics* (Oxford University Press, 2000).
50. Lim, L. H. S., Timofeeva, T. A. & Gibson, D. I. Dactylogyridae monogeneans of the siluriform fishes of the Old World. *Syst. Parasitol.* **50**, 159–197 (2001).
51. Verma, C., Chaudhary, A. & Shanker Singh, H. Redescription of two species of *Thaparocleidus* (Monogenea: Dactylogyridae) with the description of *T. armillatus* sp. n. from Wallago attu and a phylogenetic analysis based on 18S rDNA sequences. *Acta Parasitol.* **62**(3), 652–665 (2017).
52. Rajvanshi, S., Agrawal, N. & Upadhyay, M. K. *Thaparocleidus devraji* (Gusev, 1976) Lim, 1996, Infesting *Ompok bimaculatus* (Bloch, 1794) (Siluriformes: Siluridae): Morphological and Molecular Study. *AZB* **2**(2), 23–41 (2014).
53. Pandey, K. C., Agrawal, N., Vishwakarma, P. & Sharma, J. Redescription of some Indian species of *Thaparocleidus* Jain, 1952 (Monogenea), with aspects of the developmental biology and mode of attachment of *T. pusillus* (Gusev, 1976). *Syst. Parasitol.* **54**, 207–221 (2003).
54. Rajvanshi, S. & Agrawal, N. One known and an unknown species of the genus *Thaparocleidus* Jain, 1952, infecting *Sperata aor* (Hamilton, 1822): Comparison with species from China, on molecular basis. *Bioinformation* **9**(11), 577–582 (2013).
55. Kritsky, D. C., Pandey, K. C., Agrawal, N. & Abdullah, S. M. Monogenoids from the gills of spiny eels (Teleostei: Mastacembelidae) in India and Iraq, proposal of *Mastacembelocleidus* gen. n., and status of the Indian species of *Actinocleidus*, *Urocleidus* and *Haplocleidus* (Monogeneoidea: Dactylogyridae). *Folia Parasitol.* **51**(4), 291–298 (2004).
56. Narba, D., Matey, C., Agarwal, N. & Tripathi, A. A redescription and new host record for *Dactylogyryrus nasutai* Narba and Wangchu, 2015 (Platyhelminthes, Monogenea) from Arunachal Pradesh, India using high-resolution microscopy imaging. *J. Appl. Nat. Sci.* **14**(1), 188–193 (2022).
57. Wu, B. L., Long, S., Wang, W., Ma, C., Jiang, N., Chen, Z., Liu, J., Liang, R., Yao, W. & Zhao, Y. *Fauna Sinica: Invertebrata, Volume 22: Platyhelminthes: Monogenea*. Science Press, Beijing, pp 758 (2000). (In Chinese)

Acknowledgements

This project was funded by the European Union's Horizon 2020 research and innovation program under Marie Skłodowska-Curie grant agreement No. 956481. The authors are indebted to Ms. Györgyi Pataki and Ms. Natacha Leininger Severin for the histological slides. Also, thanks to Mr. Gergely Lajos Zöldi for maintaining fish in the laboratory.

Author contributions

All authors conceived the study. W.S.W.M.H., S.B, B.K., and S.C contributed to the conception and design of the study. W.S.W.M.H. and B.K., conducted the experimental procedures and analyzed the data with the assistance from K.P.W, and K.S. Writing-Original Draft, W.S.W.M.H. Review & Editing, S.B, B.K., and M.K. Figures created by W.S.W.M.H. Data interpretation and result contributed by M.K. and B.K. The research project, which received funding was initiated by S.C. The authors read and approved the final manuscript.

Funding

Open access funding provided by HUN-REN Veterinary Medical Research Institute.

Competing interests

The authors declare no competing interests.

Additional information

Supplementary Information The online version contains supplementary material available at <https://doi.org/10.1038/s41598-024-61032-3>.

Correspondence and requests for materials should be addressed to B.S.

Reprints and permissions information is available at www.nature.com/reprints.

Publisher's note Springer Nature remains neutral with regard to jurisdictional claims in published maps and institutional affiliations.



Open Access This article is licensed under a Creative Commons Attribution 4.0 International License, which permits use, sharing, adaptation, distribution and reproduction in any medium or format, as long as you give appropriate credit to the original author(s) and the source, provide a link to the Creative Commons licence, and indicate if changes were made. The images or other third party material in this article are included in the article's Creative Commons licence, unless indicated otherwise in a credit line to the material. If material is not included in the article's Creative Commons licence and your intended use is not permitted by statutory regulation or exceeds the permitted use, you will need to obtain permission directly from the copyright holder. To view a copy of this licence, visit <http://creativecommons.org/licenses/by/4.0/>.

© The Author(s) 2024